

Predicting the drying shrinkage behavior of high strength portland cement mortar under the combined influence of fine aggregate and steel micro fiber

Zhengqi Li✉

Glenn Department of Civil Engineering, Clemson University, (Clemson, United States)
✉zhengqi@clemson.edu

Received 27 April 2016
Accepted 15 September 2016
Available on line 1 March 2017

ABSTRACT: The workability, 28-day compressive strength and free drying shrinkage of a very high strength (121-142 MPa) steel micro fiber reinforced portland cement mortar were studied under a combined influence of fine aggregate content and fiber content. The test results showed that an increase in the fine aggregate content resulted in decreases in the workability, 28-day compressive strength and drying shrinkage of mortar at a fixed fiber content. An increase in the fiber content resulted in decreases in the workability and drying shrinkage of mortar, but an increase in the 28-day compressive strength of mortar at a fixed fine aggregate content. The modified Gardner model most accurately predicted the drying shrinkage development of the high strength mortars, followed by the Ross model and the ACI 209R-92 model. The Gardner model gave the least accurate prediction for it was developed based on a database of normal strength concrete.

KEYWORDS: Portland cement; Mortar; Drying shrinkage; Prediction; Steel micro fiber

Citation/Citar como: Zhengqi Li (2017) Predicting the drying shrinkage behavior of high strength portland cement mortar under the combined influence of fine aggregate and steel micro fiber. *Mater. Construcc.* 67 [326], e119. <http://dx.doi.org/10.3989/mc.2017.05916>

RESUMEN: *Predicción del comportamiento de retracción por secado de morteros de cemento Pórtland de alta resistencia bajo la influencia combinada de árido fino y micro fibra de acero.* Se ha estudiado la trabajabilidad, resistencia a la compresión (28 días) y la retracción al secado de morteros de cemento Pórtland de muy alta resistencia (121-142 MPa) reforzados con micro fibra de acero, con la influencia combinada de contenido de árido fino y de micro fibra de acero. El aumento en el contenido de árido fino resultó en la disminución de la trabajabilidad, resistencia a la compresión y la retracción por secado de los morteros con un contenido de fibra específico. El aumento en el contenido de fibra dio lugar a la disminución de la trabajabilidad y la retracción por secado, y a un aumento en la resistencia a la compresión a 28 días en morteros con un contenido específico de árido fino. El modelo modificado de Gardner predijo con más precisión la retracción por secado de mortero de alta resistencia, seguido por el modelo de Ross y el modelo ACI 209R-92. El modelo de Gardner dio la predicción menos exacta debido al hecho de que se desarrolló sobre bases de datos de hormigones de resistencia normal.

PALABRAS CLAVE: Cemento Portland; Mortero; Retracción por secado; Predicción; Micro fibra de acero

ORCID ID: Zhengqi Li (<http://orcid.org/0000-0002-7675-4525>)

Copyright: © 2017 CSIC. This is an open-access article distributed under the terms of the Creative Commons Attribution License (CC BY) Spain 3.0

1. INTRODUCTION

Steel fiber reinforced high strength portland cement mortar has been used to develop ultra-high performance concrete in the previous literature (1–7). High strength portland cement mortar with good workability, high compressive and tensile strength, and durability can be produced using low water-cementitious materials ratio, high quality fine aggregate/sand, steel reinforcing fiber and high range water reducing admixtures (HRWRA). As it is known, cementitious mixtures have the tendency to shrink (8–11). For structural concrete members restrained by adjacent members, cracks may occur due to excessive shrinkage (8–11). One type of the shrinkage of concrete is drying shrinkage which is caused by the loss of water into the environment from the hardened concrete (8).

Cement paste is the main factor influencing the drying shrinkage of concrete. The aggregate and the reinforcing fiber present in the concrete affect the drying shrinkage behavior of concrete by influencing the paste in the concrete. Some of the previous studies showed that the increase in the aggregate content reduced the drying shrinkage of concrete, which was attributed to the reduced volume of paste in the concrete and restrained paste shrinkage by the stiff aggregate particles (8, 12–16). Besides the reduced drying shrinkage, the increase in the sand content resulted in a decrease in the workability of mortar due to the large surface area of the sand particles (17, 18), and a decrease in the compressive strength of mortar due to the increased amount of the interfacial transition zone (19). It was reported in the literature that the proper use of reinforcing fiber in mortar not only restrained the crack propagation in the hardened mortar and improved the tensile strength of mortar, but also restrained the shrinkage of paste (8, 10, 20–22). However, as the reinforcing fiber content increased, a decrease in the workability of mortar was observed, and was attributed to the internal resistance and friction by the interaction of fibers (23). An increase or a decrease in the compressive strength of mortar was reported in the different literature (23–25).

Ultra-high performance concrete has been found to have higher drying shrinkage than normal strength concrete (4, 5). A study on the influence of the component materials on the drying shrinkage behavior of high strength mortar is helpful to develop methods of reducing the drying shrinkage of the ultra-high performance concrete. The previous literature was mostly focused on the effects of either the sand content or the reinforcing fiber content on the drying shrinkage of normal strength mortar/concrete (8, 10, 20–22). A study on the combined effect of the sand content and the reinforcing fiber content on the drying shrinkage behavior of fiber reinforced high strength cement mortar is desired. Models for predicting the drying shrinkage

development of high strength mortar is also of interest as the previous literature on drying shrinkage prediction was mostly focused on the normal strength mortar/concrete.

The present study was conducted to investigate the combined effect of the sand content and the steel micro fiber (SMF) content on the workability, 28-day compressive strength and free drying shrinkage development (up to 147 days) of high strength cement mortar. Prediction models for the free drying shrinkage development of high strength mortar were developed and compared with several frequently used models including the Ross model, the Gardner model, and the ACI 209R model (26–29).

2. EXPERIMENTAL PROGRAM

2.1. Materials

A Type III portland cement meeting ASTM C150 specification was used for the experimental study (30). The main chemical compositions of the cement are listed as follows: CaO 64.4%, SiO₂ 20.4%, Al₂O₃ 6%, Fe₂O₃ 3.5%, and SO₃ 3.5%. The specific gravity and Blaine's surface area of the cement were 3.15 and 540 m²/kg, respectively.

The fine aggregate was semi-round natural siliceous sand meeting the gradation specification in ASTM C33 for fine aggregates (31). The gradation is shown in Table 1. The specific gravity, water absorption, and fineness modulus of the sand were 2.63, 0.3%, and 2.65, respectively.

The steel micro fibers used were approximately 13 mm in length and 0.2 mm in diameter. Their specific gravity and ultimate tensile strength were 7.8 and 2000 MPa (290 000 psi), respectively. A powder form of polycarboxylate ether-based high-range water-reducing admixture was used to improve the workability of mortar.

2.2. Mixture proportions

In total, thirteen mortar mixtures were investigated to study the combined influence of sand content and SMF content on the properties of high

TABLE 1. Gradation of fine aggregate

Sieve opening (mm)	Percent Passing
9.5	100.0
4.75	99.8
2.36	97.1
1.18	82.0
0.60	41.9
0.30	14.0
0.15	0.5
0.075	0.1

TABLE 2. Relative proportions of materials in mortar

Mortar ID	By mass			By volume	
	c*/c*	s/c*	w/c*	HRWRA/c*	V _{SMF} /V _T
M00	1.00	0.00	0.20	0.01	0.00
M01		0.50			0.00
M02		1.25			0.00
M03		1.60			0.00
M11		0.50			0.01
M12		1.25			0.01
M13		1.60			0.01
M21		0.50			0.02
M22		1.25			0.02
M23		1.60			0.02
M31		0.50			0.03
M32		1.25			0.03
M33		1.60			0.03

Note: * cement

strength mortar. The sand content was expressed as a mass ratio of sand to cement (s/c). The sand content was investigated at levels of 0, 0.5, 1.25 and 1.6. The SMF content was expressed as a volume ratio of SMF to the total mortar mixture (V_{SMF}/V_T). The SMF content was investigated at levels of 0.00, 0.01, 0.02 and 0.03. For the entire investigation, the water-to-cement ratio (w/c) by mass was fixed at 0.2, and the HRWRA-to-cement ratio by mass was fixed at 0.01. The relative mixture proportions of the thirteen mortar mixtures are shown in Table 2.

The first mortar M00 was the control which did not contain either sand or SMF. It was basically a portland cement paste. The next 3 mortar mixtures M01, M02, and M03 were non-fiber reinforced mortars with a sand content at s/c=0.5, 1.25 and 1.6, respectively. The last 9 mortar mixtures were fiber reinforced mortars prepared by adding SMF into the mortars M01, M02, and M03 at the levels of 0.01, 0.02 and 0.03 by volume of the total mortar.

The quantities of materials used for 1 m³ of mortar are presented in Table 3.

2.3. Specimens preparation

The fresh mortars were prepared by a 0.02 m³ UNIVEX M20 planetary mixer. The mixing procedure was divided into four stages. First, cement, sand, and HRWRA were dry mixed for about 2 min at low speed (100 RPM). Second, the mixing water was added to the dry mixture. The mixing continued at low speed until the dry mixture started to behave as a fluid. The second stage took 2 to 5 min depending on the sand content and the SMF content. Third, as soon as the mortar reached fluid state, the mixing speed was increased to a medium speed (300 RPM), and the mixing continued for another 3 min.

TABLE 3. Quantities of materials used for 1 m³ of fresh mortar

Mortar ID	Constituents (kg/m ³)				
	Cement	Sand	Water	HRWRA	SMF
M00	1933	0	387	19.3	0
M01	1413	707	283	14.1	0
M02	1007	1259	201	10.1	0
M03	888	1421	178	8.9	0
M11	1399	700	280	14.0	78
M12	997	1247	199	10.0	78
M13	879	1407	176	8.8	78
M21	1385	693	277	13.9	156
M22	987	1234	197	9.9	156
M23	870	1393	174	8.7	156
M31	1371	685	274	13.7	234
M32	977	1221	195	9.8	234
M33	862	1379	172	8.6	234

Fourth, the SMF was added, and the mixing continued for another 3 min at the medium speed (300 RPM). The entire mixing procedure took about 10 to 13 min. The workability of mortar was measured immediately after the mixing.

The fresh mortars exhibiting self-consolidating consistency were cast into molds without vibration, while the fresh mortars exhibiting very low workability were cast into molds with external vibration for 15 seconds on a vibrating table. After casting, the specimens were kept in a moist room maintained at 100% relative humidity and 23 °C in accordance with the ASTM C511 (32). For the study of compressive strength of mortar, the specimens were demolded at 24 hours after casting, and stored in the moist room until the age of 28 days. For the study of free drying shrinkage of mortar, the specimens were de-molded at 48 hours after casting. The reason for demolding at 48 hours after casting was that the present study was a part of a broad research on the properties of mortar under the influence of various sand contents, SMF contents, different pozzolans, and different chemical admixtures. When a fly ash or a liquid form shrinkage reducing admixture was used, the compressive strength of mortar at 24 hours after casting was very low (i.e. 6 MPa), even at a water-to-cementitious materials ratio of 0.2. Those specimens had to be demolded at the age of 48 hours. To keep the test procedure consistent in the broad research, all of the specimens for the drying shrinkage test including the specimens presented in this study were demolded at the age of 48 hours. After demolding, the drying shrinkage specimens were cured in a lime-saturated water bath as per ASTM C596 (33). At the age of 72 hours after casting, the specimens were taken out of the lime-saturated water bath and their length readings

were taken (readings at zero time of measurement). Afterward, the specimens were stored in an environment chamber which was maintained at 23 ± 2 °C and $50\pm 4\%$ relative humidity in accordance with ASTM C157 (34).

2.4. Test methods

Workability

As some of the mortar mixtures exhibited very high workability, the workability of the thirteen mortar mixtures was determined by following a modified test procedure from the one described in the ASTM C1437 (35). In this modified method, the fresh mortar was filled into the flow mold with dimensions described in the ASTM C230 (36). After the flow mold was removed, the fresh mortar was allowed to spread freely on a level plastic plate, instead of being dropped for 25 times. When the mixture stopped spreading (about 5 min after the removal of the flow mold) the diameter of the circular mortar spread was measured for calculating the flow value as described in the ASTM C1437 (35).

Compressive strength

The compressive strength of each of the mortar mixtures was determined by testing three $50\times 50\times 50$ mm cubes at the ages of 28 days in accordance with the ASTM C109 (37).

Free drying shrinkage

Three specimens with dimensions of $25\times 25\times 285$ mm were prepared for each of the mortar mixtures. The length comparator readings of each specimen stored in the environmental chamber were taken following the procedures described in the ASTM C596 at the periods of exposure of 0, 1, 4, 11, 18, 25, 56, 87, 117 and 147 days (33). The drying shrinkage value of each mortar mixture at each period of

exposure was the average drying shrinkage value of the three specimens.

3. RESULTS AND DISCUSSIONS

3.1. Material properties of mortars

The mortars M11, M21 and M31 visually exhibited severe segregation of SMF, as the cement mortar spread into a circular shape quickly, while the SMF clumped at the center part of this circular shape during the workability test. The rest of the mortar mixtures did not visually show segregation of SMF as the mixtures spread into a circular shape with SMF evenly distributed. It was observed that with a SMF content up to $V_{SMF}/V_T = 0.03$, a minimum sand content at $s/cm = 1.25$ was required to prevent severe segregation of SMF. It is considered that the sand particles behaved as supports for SMF in the fresh mortar. At a sand content of $s/c = 0.5$, segregation of SMF occurred as there were not enough sand particles to support the SMF. The properties of the mortars M11, M21 and M31 are not presented here due to the severe segregation of SMF.

The workability (flow), 28-day compressive strength (CS-28), coefficient of variation of the 28-day compressive strength (COV-28), and drying shrinkage at the period of exposure of 147 days (DS-147) of the rest ten mortar mixtures are presented in Table 4. The sand content by mass of cement (s/c), sand content by volume of total mortar (V_s/V_T) and SMF content by volume of total mortar (V_{SMF}/V_T) in each mortar mixture are presented in Table 4 as well. The volume fraction of HRWRA in mortar is ignored, as the value is very small.

As shown in Table 4, the flow of mortar decreased with the increase in the sand content at a fixed SMF content. For instance, at $V_{SMF}/V_T = 0$, the flow of the mortars M01, M02, and M03 was 7%, 25% and 43% lower than that of the control mortar M00, respectively. This was attributed to the large surface area of the sand particles which

TABLE 4. Material properties of SMF reinforced high strength mortar

Mortar ID	Flow (%)	CS-28 (MPa)	COV-28 (%)	DS-147 (%)	s/c	V_s/V_T	V_{SMF}/V_T
M00	288	135.3	4.0	-0.2023	0.0	0.000	0.00
M01	269	128.3	2.2	-0.1077	0.5	0.269	0.00
M02	217	124.7	6.6	-0.0687	1.25	0.479	0.00
M03	163	121.2	2.5	-0.0567	1.6	0.540	0.00
M12	194	124.9	2.5	-0.0660	1.25	0.474	0.01
M13	156	120.7	4.5	-0.0497	1.6	0.535	0.01
M22	178	131.6	3.0	-0.0563	1.25	0.469	0.02
M23	75	122.0	6.3	-0.0467	1.6	0.530	0.02
M32	122	137.4	5.6	-0.0527	1.25	0.464	0.03
M33	13	142.4	6.2	-0.0480	1.6	0.524	0.03

reduced the amount of paste lubricating the sand particles (17, 18). The flow of mortar also decreased with the increase in the SMF content at a fixed sand content. For instance, at $s/c=1.25$, the flow of the mortars M12, M22 and M32 was 11%, 18% and 44% lower than that of the mortar M02, respectively. Likely, the internal resistance and friction resulted from the interaction of fibers were the reasons of the decreased workability as the SMF content increased (23). The mortar mixtures M23 and M33 presented very low workability. They were cast into molds with external vibration for 15 seconds to prepare the specimens for the tests of compressive strength and free drying shrinkage of the mortar mixtures. The other eight mortar mixtures which did not exhibit severe segregation of SMF were cast into molds without external vibration.

The average 28-day compressive strength of mortar decreased with the increase in the sand content at a fixed SMF content, except when V_{SMF}/V_T was 0.03. When V_{SMF}/V_T was 0, a calculation revealed that the 28-day compressive strength of the mortars M01, M02, and M03 was 5%, 8%, and 10% lower than that of the control mortar M00, respectively. This was attributed to the increased amount of the interfacial transition zone in the mortar as the sand content increased (19). However, when V_{SMF}/V_T was 0.03, the increase in the sand content actually resulted in a slight increase in the compressive strength. This was attributed to either the large variance of the measured 28-day compressive strength of the mortars M32 and M33, or the external vibration applied during casting the specimens of the mortars M23 and M33. At a fixed sand content, the increase in the SMF content up to $V_{SMF}/V_T = 0.01$ did not result in a significant increase in the 28-day compressive strength of mortar. When SMF content was higher than $V_{SMF}/V_T = 0.01$, the increase in the SMF content resulted in a significant increase in the 28-day compressive strength of mortar. For instance, at $s/c = 1.25$, the 28-day compressive strength of the mortars M12, M22 and M32 was 0.2%, 6%, and 10% higher than that of the mortar M02, respectively. The restrained crack propagation in the hardened mortar due to the use of SMF contributed to the increased compressive strength of mortar (8; 10; 20–22). It should be noted that the use of sand or SMF presented relatively limited impact on the 28-day compressive strength of portland cement mortar, compared with their significant impact on the workability of mortar.

The drying shrinkage of mortar at the period of exposure of 147 days generally decreased with the increase in the sand content when the SMF content was fixed. For instance, when V_{SMF}/V_T was 0.0, the drying shrinkage of the mortars M01, M02, and M03 was 47%, 66% and 72% lower than that of the mortar M00, respectively. This was attributed to the reduced volume of paste and the restrained

shrinking of paste by sand particles (8, 12–16). The increase in the SMF content generally resulted in a decrease in the drying shrinkage of mortar at the period of exposure of 147 days when the sand content was fixed. For instance, when s/c was 1.25, the drying shrinkage of the mortars M12, M22 and M32 was 4%, 18% and 23% lower than that of the mortar M02, respectively. This was likely due to the restrained shrinkage of paste by the fibers (8; 10; 20–22). Moreover, the increase in the SMF content also resulted in the reduction of paste volume in the mortar, which contributed to the reduced drying shrinkage to a small extent. It should be noticed that the drying shrinkage of the mortar M33 was higher than that of the mortar M23. This did not follow the general trend discussed above and was likely attributed to the external vibration applied during casting the mortars M23 and M33.

From the consideration of reducing the drying shrinkage of high strength, it was preferable to increase the sand content or the SMF content in the mortar mixture. However, the increase in the sand content resulted in a decrease in both the workability and the compressive strength of mortar, and the increase in the SMF content resulted in a decrease in the workability of mortar as well. Considering that SMF may increase the compressive strength of mortar, a properly used combination of the sand content and the SMF content may lower the drying shrinkage of mortar and overcome the strength reduction effect of increasing sand content, and at the same time maintain a workable consistency of mortar. As discussed previously, the mortars M23 and M33 exhibited very low workability. An external vibration was applied for consolidation during casting. This indicated that at a sand content of $s/c = 1.6$, the maximum SMF volume content could be achieved while maintaining a self-consolidating consistency of mortar was $V_{SMF}/V_T = 0.01$. Mortar M32 exhibited good workability. This indicated that at a sand content of $s/c = 1.25$, the SMF volume content as high as $V_{SMF}/V_T = 0.03$ could be used in the mortar without resulting in a very low workability of mortar. Although the optimal maximum value of the sand content and the SMF content from the consideration of maintaining a self-consolidating workability while achieving a low drying shrinkage was not investigated, it was considered that, at sand content of $s/c = 1.25$ and $s/c = 1.6$, the maximum SMF content in mortar could go up to $V_{SMF}/V_T = 0.03$ and $V_{SMF}/V_T = 0.01$, respectively.

The drying shrinkage development of the ten mortar mixtures is presented in Figure 1.

As shown in Figure 1, the drying shrinkage of mortar after the period of exposure of 117 days did not change significantly. The experimental drying shrinkage values of mortars at the period of exposure of 147 days were considered the ultimate drying shrinkage. It should be noted that most of the drying

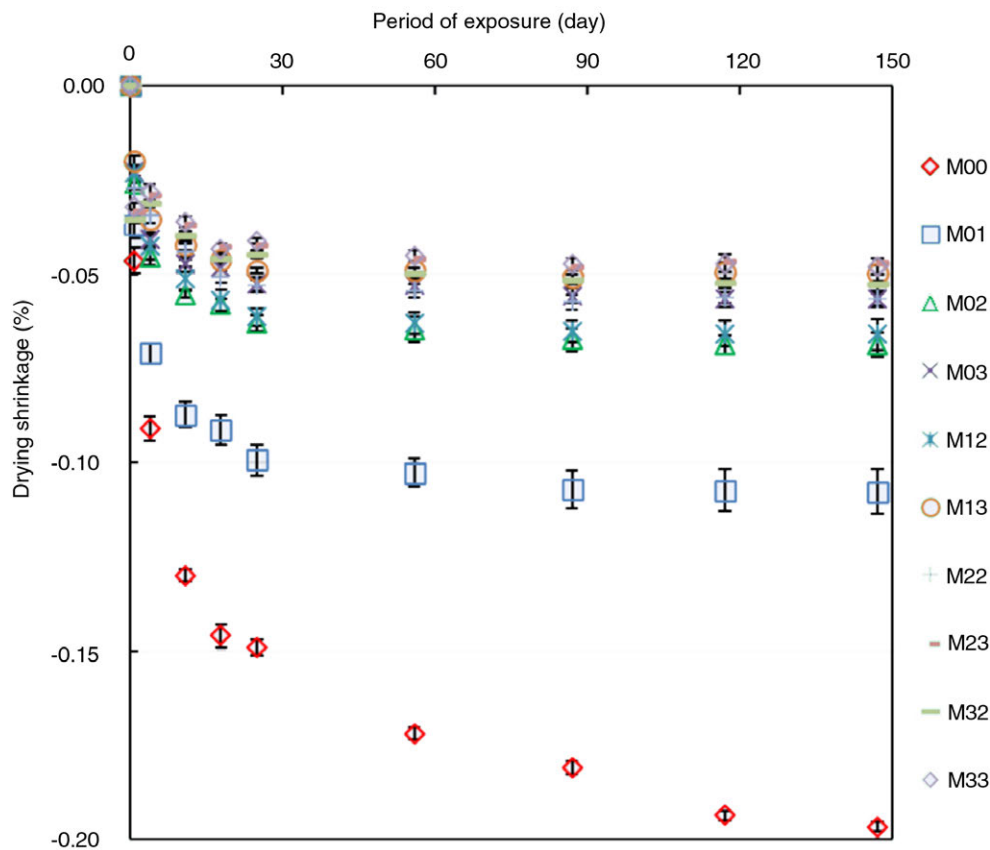


FIGURE 1. Drying shrinkage development of SMF reinforced high strength mortar.

shrinkage of high strength mortar presented in this study was larger than that of most of the normal strength mortar/concrete at similar periods of exposure (8–12, 14, 15, 20–22). The high paste content in high strength mortar was considered the main reason (8, 12–16). In the later part of the present study, a regression model of predicting the ultimate drying shrinkage of mortar based on the sand content and SMF content was developed through analyzing the experimental drying shrinkage values of mortars at the period of exposure of 147 days.

3.2. Prediction of drying shrinkage development of steel fiber reinforced mortar

3.2.1. Prediction models

Four shrinkage prediction models which included three existing models in the literature and one modified model proposed in this study were used to predict the drying shrinkage development of mortar. In the prediction models, the independent variable was the period of exposure noted as t (Unit: days), and the dependent variable was drying shrinkage of mortar at a specific period of exposure noted as $\varepsilon_{sh}(t)$ (Unit: %). The predictions of drying shrinkage of mortar by these four models were compared.

The four drying shrinkage prediction models are listed in Table 5.

The Ross model and the ACI 209R-92 model both required the information of the ultimate drying shrinkage of the mixture. In the present study, the experimentally measured drying shrinkage of mortar at the period of exposure of 147 days was used as the ultimate drying shrinkage for predicting the drying shrinkage development of mortar by these two models. The Gardner model provided the prediction model of the ultimate drying shrinkage of the mixture. Noting that the prediction model of the ultimate drying shrinkage in the Gardner model was developed mainly based on the database of normal strength concrete (26; 29), it might not be proper to predict the ultimate drying shrinkage of high strength mortar. Thus, a regression equation for predicting the ultimate drying shrinkage of high strength mortar was developed (based on the experimentally measured drying shrinkage values of mortars at the period of exposure of 147 days) and used to replace the prediction model of the ultimate drying shrinkage in the Gardner model. This led to the modified Gardner model.

Before developing the regression model for predicting the ultimate drying shrinkage of high strength mortar, it was noted that the two main effects of sand and SMF on the drying shrinkage

TABLE 5. Shrinkage prediction models

Model Name	Expression	Note
Ross model (27; 28)	$\epsilon_{sh}(t) = \frac{t}{Ns + t} \epsilon_{sh\infty}$ $Ns = 0.33 \exp(0.522V/S) \text{ for } V/S \leq 7.6 \text{ mm}$	V/S: specimen's volume-surface ratio (5.987 mm)
ACI 209R-92 model (26)	$\epsilon_{sh}(t) = \frac{t^\alpha}{f + t^\alpha} \epsilon_{sh\infty}$ $f = 26 \exp(0.014V/S)$	$\alpha = 1$ V/S: specimen's volume-surface ratio (5.987 mm)
Gardner model (26; 29)	$\epsilon_{sh}(t) = -\beta(h)\beta(t)\epsilon_{sh\infty}$ $\beta(h) = 1 - 1.18h^4$ $\beta(t) = \left(\frac{t}{t + 0.15(V/S)^2} \right)^{0.5}$ $\epsilon_{sh\infty} = 1000 \times 1.15 \left(\frac{30}{f_{cm28}} \right)^{0.5} \cdot 10^{-6}$	h: relative humidity (50%) V/S: specimen's volume-surface ratio (5.987 mm) f_{cm28} : 28-day compressive strength, see Table 4
Modified Gardner model	$\epsilon_{sh\infty}$ is calculated by regression analysis	

behavior of mortars included reducing the volume of paste and restraining the drying shrinkage of paste. These two effects were closely related to the volumetric sand content and the volumetric SMF content in mortar. The higher the volume of sand or SMF was included, the less volume of paste was presented in mortar, and the more the restraining effect was applied on the drying shrinkage of the paste. Thus, the regression model for predicting the ultimate drying shrinkage of mortar was developed based on two independent variables, the sand content by volume of the total mortar which was expressed as *s*, and the SMF content by volume of the total mortar which was expressed as *f*. For each mortar mixture, the sand content by volume and the SMF content by volume are shown in Table 4. The model terms included in the least squares analysis were *s*, *s*², *s*³, *f*, *f*², *f*³ and *s*×*f*. The student's *t* test was conducted to test the null hypothesis that the estimated coefficient of each of the model terms equaled zero (38). The alternative hypothesis was that the estimated coefficient of each of the model terms did not equal zero. Only the model terms with a *p*-value of *t* test less than 0.05 were considered having statistically significant effect in the regression model. The final regression equations only included the statistically significant model terms. The regression equation is given in equation [1]:

$$\epsilon_{sh\infty} = (-0.2018 + 0.4164s - 0.2758s^2 + 0.4811f) \times 100\% \quad [1]$$

The adjusted coefficient of determination (*R*²-adjusted) for this regression equation was 0.9955. When no sand and SMF was incorporated in the mortar (*s* = 0, *f* = 0), the calculated value

-0.2018% was the prediction of the ultimate drying shrinkage of the pure portland cement paste (Mortar M00). It should be noted that equation [1] was developed based on the drying shrinkage test results of mortars with a w/c at 0.2. It was likely this equation was not valid for mortars with w/c rather than 0.2, as the w/c was one of the major factors affecting the drying shrinkage behavior of mortar.

The predictions of the drying shrinkage development of mortar by the four models are summarized as follows: For the Ross model and the ACI 209R-92 model, the experimentally measured drying shrinkage of mortar at the period of exposure of 147 days was used as the ultimate drying shrinkage for predicting the drying shrinkage development of mortar; For the Gardner model, the ultimate drying shrinkage of mortar was calculated by the equation presented in the Gardner model; For the modified Gardner model, the ultimate drying shrinkage of mortar was calculated by equation [1], which was used afterward to predict the drying shrinkage development of mortar.

3.2.2. Comparison of the prediction models

For each of the four prediction models, the predicted drying shrinkage values are plotted against the experimentally measured drying shrinkage values of each of the ten mortar mixtures at the periods of exposure of 0, 1, 4, 11, 18, 25, 56, 87, 117 and 147 days (See Figure 2). Thus, each plot in Figure 2 includes 100 data points. A linear regression equation is also developed to show the relation between the predicted drying shrinkage and the experimentally measured drying shrinkage of mortar. This figure gives visual information about the effectiveness

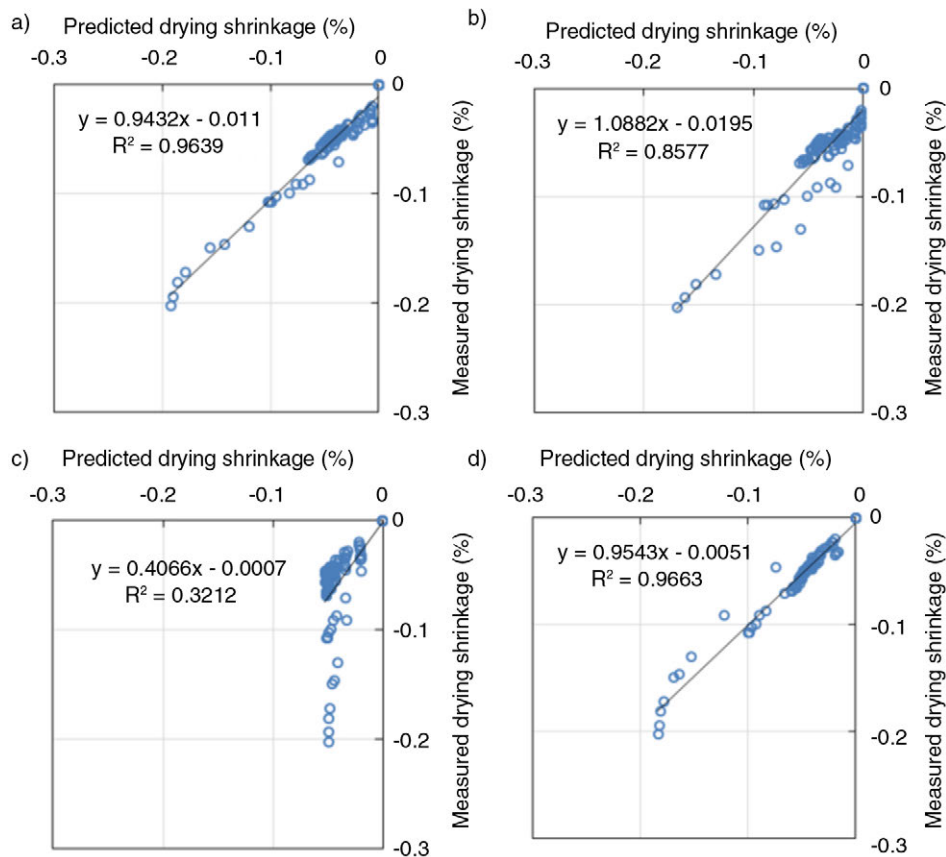


FIGURE 2. Relation between predicted drying shrinkage and measured average drying shrinkage.

TABLE 6. Coefficient of determination of each of the four models for predicting the drying shrinkage of mortar

Models	Ross model	ACI 209R-92 model	Gardner model	Modified Gardner model
R^2	0.9154	0.5254	0.1171	0.9596

of the four models in predicting the drying shrinkage development of SMF reinforce mortar.

If the predicted drying shrinkage values ideally match the experimentally measured drying shrinkage values, the relation between predicted drying shrinkage and the measured drying shrinkage shall follow the equation $y(x) = x$ where x is the predicted drying shrinkage and $y(x)$ is the measured drying shrinkage. The linear regression equations in Figure 2 visually indicate if the relation between the predicted drying shrinkage and the measured drying shrinkage is close to equation $y(x) = x$. Based on the slope and the interception of the linear regression equation of the relation between the predicted drying shrinkage and the experimentally measured drying shrinkage, the modified Gardner model most accurately predict the drying shrinkage development of mortar, as the slope and the interception were very close to 1 and 0, respectively, and the coefficient of determination (R^2) was as high as 0.9663. The Ross model appeared to be a good model, as the

slope and the interception were very close to 1 and 0, respectively, and the R^2 was as high as 0.9639. The ACI 209R-92 model was not as good as either the modified Gardner model or the Ross model, as its R^2 was lower than that of the modified Gardner model and the Ross model. The Gardner model did not give a good prediction, as the slope of the linear regression equation was significantly different from 1, and the R^2 was small.

To have a direct comparison of the four prediction models, the coefficient of determination indicating the effectiveness of the model replicating the observed drying shrinkage development was calculated and presented in Table 6. The calculation of the coefficient of determination of each model was based on the predicted drying shrinkage and the experimentally measured drying shrinkage of each of the ten mortar mixtures at the periods of exposure of 0, 1, 4, 11, 18, 25, 56, 87, 117 and 147 days. Thus, the coefficient of determination of each model shown in Table 6 was calculated based on the

200 data points (100 experimental data and 100 predicted data).

By comparing the value of R^2 , the modified Gardner model was found to be the most accurate in predicting the drying shrinkage of mortar, indicated by a R^2 of 0.9596. The Ross model was a good model with a R^2 of 0.9154. The ACI 209R-92 model was not as good as the Ross model or the modified Gardner model, indicated by a R^2 of 0.5254. It should be noted that both the Ross model and the ACI 209R-92 model required the input of the ultimate drying shrinkage of mortar for calculation, while the modified Gardner model provided a prediction of the ultimate drying shrinkage of mortar ($w/c = 0.2$) for calculation based on the sand content and the SMF content. The Gardner model give the least accurate prediction of the drying shrinkage of mortar, indicated by a low R^2 of 0.1171. This was likely due to the fact that the predictions of ultimate drying shrinkage in the Gardner model was based on a database of normal strength concrete (26; 29), and it was not proper for predicting the ultimate drying shrinkage of high strength mortar. Another point of interest was that the mathematical expression of the Gardner model consisted of two parts: one part determined the ultimate drying shrinkage of concrete, and another part determined the shape of the drying shrinkage development curve. The comparison of the Gardner model and the modified Gardner model revealed that the part determining the shape of the drying shrinkage development curve in the Gardner model still worked well for SMF reinforced high strength cement mortar.

It should be noted that the modified Gardner model is validated by the measured drying shrinkage data of mortar presented in this study with 28-day compressive strength ranging from 121 MPa to 142 MPa. It has not been validated by test results from other researchers' studies due to the limited previous literature on the mortars at such high strength level. More study is needed to accommodate the modified Gardner model to a wide range of mortars.

4. CONCLUSIONS

In this study, the workability, 28-day compressive strength and free drying shrinkage of a very high strength (121-142 MPa) steel fiber reinforced cement mortar were investigated. Prediction equations for the drying shrinkage development of steel fiber reinforced high strength mortar with a w/c at 0.2 were developed. The results presented in this study contributed to the existing knowledge of concrete by focusing on the combined influence of sand content and fiber content on the properties of high strength mortar. A method to predict the drying shrinkage behavior of high strength mortar was proposed in this study as well. Based on the materials,

proportions and test methods used in this study, the following conclusions were drawn:

- The increase in the sand content resulted in a significant decrease in the workability of high strength cement mortar at a fixed SMF content. The increase in the SMF content resulted in a decrease in the workability of mortar at a fixed sand content.
- The increase in the sand content generally resulted in a slight decrease in the 28-day compressive strength of high strength cement mortar at a fixed SMF content. The large variance of test results and the external vibration applied during casting the mortar M33 were considered reasons for the exception when SMF content was $V_{SMF}/V_T = 0.03$. The 28-day compressive strength of mortar was not significantly increased by increasing the SMF content up to $V_{SMF}/V_T = 0.01$. When SMF content was higher than $V_{SMF}/V_T = 0.01$, the increase in the SMF resulted in a significant increase in the 28-day compressive strength of high strength cement mortar.
- The increase in the sand content or the SMF content generally resulted in a decrease in the drying shrinkage of high strength cement mortar. The drying shrinkage of the mortar M33 was higher than that of the mortar M23, which did not follow such general trend. This was attributed to the external vibration applied during casting the mortars M23 and M33.
- The ultimate drying shrinkage of high strength mortar with a w/c at 0.2 was well predicted simply based on the volumetric sand content and the volumetric SMF content in the mortar mixture. The regression equation had a R^2 -adjust as high as 0.9955.
- The modified Gardner model most accurately predicted the drying shrinkage development of high strength mortar, followed by the Ross model. The ACI 209R-92 model was not as good as the Ross model and the modified Gardner model. The existing Gardner model gave the least accurate prediction of the drying shrinkage development of steel micro fiber reinforced high strength cement mortar. This is likely due to the fact that it was developed based on a database of normal strength concrete.

REFERENCES

1. Yu, R.; Spiesz, P.; Brouwers, H. J. H. (2015) Development of an eco-friendly Ultra-High Performance Concrete (UHPC) with efficient cement and mineral admixtures uses. *Cem. Concr. Compos.*, 55, 383–394. <https://doi.org/10.1016/j.cemconcomp.2014.09.024>
2. Magureanu, C.; Sosa, I.; Negrutiu, C.; Heghes, B. (2012) Mechanical Properties and Durability of Ultra-High-Performance Concrete. *ACI Mater. J.*, 109 [2], 177–183.

3. Tafrroui, A.; Escadeillas, G.; Lebailli, S.; Vidal, T. (2009) Metakaolin in the formulation of UHPC. *Constr. Build. Mater.*, 23 [2], 669–674. <https://doi.org/10.1016/j.conbuildmat.2008.02.018>
4. Graybeal, B. A. (2006) Material property characterization of ultra-high performance concrete. Report FHWA-HRT-06-103: U.S. Department of Transportation. Washington D.C. (2006).
5. Li, Z.; Kizhakommudom, H.; Rangaraju, P. R.; Schiff, S. D. (2014) Development of ultra-high performance concrete for shear-keys in precast bridges using locally available materials in South Carolina. Proceedings of 2014 60th Anniversary Convention and National Bridge Conference, Washington, D.C., (2014).
6. ACI 201.2R-08. (2008) Guide to Durable Concrete. American Concrete Institute. Farmington Hills, Michigan, (2008).
7. Wille, K.; Boisvert-Cotulio, C. (2013) Development of Non-Proprietary Ultra-High Performance Concrete for Use in the Highway Bridge Sector. Report FHWA-HRT-13-100. FHWA, U.S. Department of Transportation. Washington, D.C., (2013).
8. Mindess, S.; Young, J. F.; Darwin, D. (2003) Concrete. Prentice Hall, Pearson Education, Inc. Upper Saddle River, New Jersey, (2003).
9. Sargaphuti, M.; Shah, S.; Vinson, K. (1993) Shrinkage cracking and durability characteristics of cellulose fiber reinforced concrete. *ACI Mater. J.*, 90 [4], 309–318.
10. Grzybowski, M.; Shah, S. P. (1990) Shrinkage cracking of fiber reinforced concrete. *ACI Mater. J.*, 87 [2], 138–148.
11. Zhang, W.; Zakaria, M.; Hama, Y. (2013) Influence of aggregate materials characteristics on the drying shrinkage properties of mortar and concrete. *Constr. Build. Mater.*, 49, 500–510. <https://doi.org/10.1016/j.conbuildmat.2013.08.069>
12. Odman, S. (1968) Effects of variations in volume, surface area exposed to drying, and composition of concrete on shrinkage. *Le Retrait des Betons Hydrauliques*, Madrid (1968).
13. Li, Z.; Rangaraju, P. R. (2015) Effect of Sand Content on the Properties of Self-Consolidating High Performance Cementitious Mortar. *Transport. Res. Rec.*, 2508, 84–93. <https://doi.org/10.3141/2508-11>
14. Hansen, T. C.; Nielsen, K. E. (1965) Influence of aggregate properties on concrete shrinkage. *ACI Journal Proceedings*. (1965).
15. Hobbs, D. (1974) Influence of aggregate restraint on the shrinkage of concrete. *ACI Journal Proceedings*, (1974).
16. Idiart, A.; Bisschop, J.; Caballero, A.; Lura, P. (2012) A numerical and experimental study of aggregate-induced shrinkage cracking in cementitious composites. *Cem. Concr. Res.*, 42 [2], 272–281. <https://doi.org/10.1016/j.cemconres.2011.09.013>
17. Li, L. G.; Kwan, A. K. H. (2011) Mortar design based on water film thickness. *Constr. Build. Mater.*, 25 [5], 2381–2390. <https://doi.org/10.1016/j.conbuildmat.2010.11.038>
18. Reddy, B. V. V.; Gupta, A. (2008) Influence of sand grading on the characteristics of mortars and soil-cement block masonry. *Constr. Build. Mater.*, 22 [8], 1614–1623. <https://doi.org/10.1016/j.conbuildmat.2007.06.014>
19. Scrivener, K. L.; Gariner, E. M. (1988) Microstructural Gradients in Cement Paste around Aggregate Particles. *Material Research Symposium Proceedings*, (1988).
20. Juarez, C.; Fajardo, G.; Monroy, S.; Duran-Herrera, A.; Valdez, P.; Magniont, C. (2015) Comparative study between natural and PVA fibers to reduce plastic shrinkage cracking in cement-based composite. *Constr. Build. Mater.*, 91, 164–170. <https://doi.org/10.1016/j.conbuildmat.2015.05.028>
21. Voigt, T.; Bui, V. K.; Shah, S. P. (2004) Drying shrinkage of concrete reinforced with fibers and welded-wire fabric. *ACI Mater. J.*, 101 [3], 233–241.
22. Bandelj, B.; Saje, D.; Jacob, S. (2011) Free shrinkage of high performance steel fiber reinforced concrete. *J. Therm. Anal.*, 39 [2], 1–11.
23. Emdadi, A.; Mehdipour, I.; Libre, N. A.; Shekarchi, M. (2015) Optimized workability and mechanical properties of FRCM by using fiber factor approach: theoretical and experimental study. *Mater. Struct.*, 48 [4], 1149–1161. <https://doi.org/10.1617/s11527-013-0221-3>
24. Nehdi, M.; Ladanchuk, J. D. (2004) Fiber synergy in fiber-reinforced self-consolidating concrete. *ACI Mater. J.*, 101 [6], 508–517.
25. Banthia, N.; Gupta, R. (2004) Hybrid fiber reinforced concrete (HyFRC): fiber synergy in high strength matrices. *Mater. Struct.*, 37 [274], 707–716. <https://doi.org/10.1007/BF02480516>
26. ACI 209. (2008) Guide for Modeling and Calculating Shrinkage and Creep in Hardened Concrete. American Concrete Institute. Farmington Hills, Michigan, (2008).
27. Ross, A.D. (1944) Shape, Size and Shrinkage. *Concr. Constr. Eng.*, 39 [8], 193–199.
28. Almudaiheem, J. A.; Hansen, W. (1987) Effect of Specimen Size and Shape on Drying Shrinkage of Concrete. *ACI Mater. J.*, 84 [2], 130–135.
29. Gardner, N.; Lockman, M. (2001) Design provisions for drying shrinkage and creep of normal-strength concrete. *ACI Mater. J.*, 98 [2], 159–167.
30. ASTM C150. (2015) Standard Specification for Portland Cement. ASTM International. West Conshohocken, Pennsylvania, (2015).
31. ASTM C33. (2013) Standard Specification for Concrete Aggregates. ASTM International. West Conshohocken, Pennsylvania, (2013).
32. ASTM C511. (2013) Standard Specification for Mixing Rooms, Moist Cabinets, Moist Rooms, and Water Storage Tanks Used in the Testing of Hydraulic Cements and Concretes. ASTM International. West Conshohocken, Pennsylvania, (2013).
33. ASTM C596. (2009) Standard Test Method for Drying Shrinkage of Mortar Containing Hydraulic Cement. ASTM International. West Conshohocken, Pennsylvania, (2009).
34. ASTM C157. (2014) Standard Test Method for Length Change of Hardened Hydraulic-Cement Mortar and Concrete. ASTM International. West Conshohocken, Pennsylvania, (2014).
35. ASTM C1437. (2013) Standard Test Method for Flow of Hydraulic Cement Mortar. ASTM International. West Conshohocken, Pennsylvania, (2013).
36. ASTM C230. (2014) Standard Specification for Flow Table for Use in Tests of Hydraulic Cement. ASTM International. West Conshohocken, Pennsylvania, (2014).
37. ASTM C109. (2013) Standard test method for compressive strength of hydraulic cement mortars (Using 2-in. or [50-mm] cube specimens). ASTM International. West Conshohocken, Pennsylvania, (2013).
38. Ott, R. L.; Longnecker, M. (2010) *An Introduction to Statistical Methods and Data Analysis* (Sixth ed.). Brooks/Cole, Cengage Learning. Belmont, California (2010).